Interactions between the Donor and Acceptor Sides in Bacterial Reaction Centers[†]

Nicolas Ginet and Jérôme Lavergne*

CEA-DEVM/LBC, Cadarache, 13108 Saint Paul-lez Durance, France

Received July 7, 2000; Revised Manuscript Received September 27, 2000

ABSTRACT: The apparent equilibrium constant K'_2 for electron transfer between the primary (Q_A) and secondary (Q_B) quinone acceptors of the reaction center was measured in chromatophores of *Rhodobacter capsulatus*. In the presence of the oxidized primary donor P^+, we obtained a value of $K'_2(P^+) \approx 100$ at pH 7.2, based on the rates of recombination from $P^+Q_A^-$ and $P^+Q_B^-$. K'_2 was also measured in the presence of reduced P, from the damping of semiquinone oscillations during a series of single turnover flashes. A 5-fold smaller value, $K'_2(P) \approx 20$, was found. Additional information on the interactions between the donor and acceptor sides was obtained by measuring the shift of the midpoint potential of P caused by the presence of Q_B^- or Q_A^-S (where S indicates the presence of the inhibitor stigmatellin). A stabilization of the oxidized state P^+ was observed in both instances, by 10 mV for Q_B^- and 30 mV for Q_A^-S. The larger stabilization of $P^+Q_A^-S$ with respect to $P^+Q_B^-$ does not account for the effect of P^+/P on K'_2. Analysis of these results indicates that the interactions between P^+/P and Q_A/Q_A^- are markedly modified depending on the occupancy of the Q_B pocket by ubiquinone or by stigmatellin. We propose that the large value of $K'_2(P^+)$ results essentially from a conformational destabilization of the $P^+Q_A^-$ state, that is relieved when the proximal site of the Q_B pocket is occupied by stigmatellin.

The bacterial reaction center is the best known membrane protein complex to date and has become a paradigm for understanding biological electron transfer. Accurate three-dimensional structures are available (*1*), together with a wealth of spectroscopic investigations on both the native complex and variants obtained from site-directed mutagenesis. An intriguing question is whether the protein is only providing the appropriate scaffold for a precise location of redox centers and tuning of their energy levels and reorganization energies or, in addition, undergoes structural changes which may concur to the energetic performance of the system. There has been a number of reports showing evidence for conformational changes in response to charge separation. For instance, when immobilizing the RC[1] in the $P^+Q_A^-$ state, either by chemical cross-liking (*2*) or by freezing (*3*), the recombination kinetics are markedly modified. An electrogenic response following charge separation in the 100 μs domain has been reported, in the absence of any concomitant electron transfer (*4*). Marked modifications of the binding properties of the Q_B pocket have been observed, depending on the redox state of the primary quinone acceptor (*5*, *6*). These concern the binding of neutral species (ubiquinone or inhibitors) and cannot simply be due to an electrostatic effect. A movement of the secondary quinone involving displacement and turnover of the quinone ring (from a "distal" to a "proximal" configuration) is believed to accompany the formation of the semiquinone state Q_B^- (*7*−*9*). In the present paper, we investigate the interactions between the primary donor P and the quinone acceptors, Q_A and Q_B, mainly in chromatophores from *R. capsulatus*, and show that, in addition to an electrostatic contribution, some conformational constraint must be involved.

The reactions of interest here involve the primary photochemical electron donor P (special pair of bacteriochlorophylls) and the primary and secondary ubiquinone acceptors Q_A and Q_B. Whereas Q_A is a single electron carrier, Q_B undergoes sequentially a first reduction to the semiquinone state Q_B^- and a second reduction, accompanied by the binding of two protons, to the quinol state Q_BH_2. In the fully oxidized (quinone) and fully reduced state (quinol), the secondary quinone is weakly attached to its binding site (the Q_B pocket) and undergoes rapid exchange with the ubiquinones of the pool solubilized in the membrane lipid phase. In contrast, the semiquinone Q_B^- is strongly bound to the protein and can remain thus stabilized on a long time scale (e.g., minutes). The two-electron cycle of the secondary quinone (see ref *10* for a review) is summarized below:

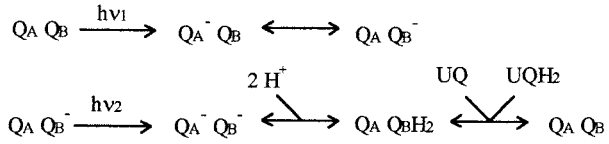

where $h\nu_1$ and $h\nu_2$ denote two successive photoacts. The photochemical charge separation $PQ_A \rightarrow P^+Q_A^-$ implies the presence of the reduced primary donor P and oxidized Q_A. A secondary donor (such as cytochrome c_2 in vivo) is thus required for reducing P^+ and allows completion of the above cycle. In the absence of a secondary donor, light induces the state $P^+Q_AQ_B^-$ which back reacts in the seconds time

[†] This work was supported by the CEA and CNRS.

* To whom correspondence should be addressed. Phone: +33 4 42 25 45 80. Fax: +33 4 42 25 47 01. E-mail: jerome.lavergne@cea.fr.

[1] Abbreviations: Bphe, bacteriopheophytin; Q_A, Q_B, primary or secondary quinone acceptor; RC, reaction center; *R*, *Rhodobacter*; TMPD, *N*,*N*,*N*′,*N*′-tetramethyl-1,4-phenylenediamine; UQ, ubiquinone.

10.1021/bi001588p CCC: $19.00
Published on Web 11/29/2000

range, restoring the initial state PQ_AQ_B. This back reaction involves two competing routes, namely a direct electron transfer from Q_B^- to P^+ and an indirect pathway where the recombination reaction occurs from Q_A^- to P^+ through the electron-transfer equilibrium $Q_AQ_B^- \leftrightarrow Q_A^-Q_B$ (*11*−*15*). The latter process is generally dominant so that the rate of the observed recombination is controlled by the equilibrium constant $K_2' = [Q_AQ_B^-]/[Q_A^-*]$. In this expression $[Q_A^-*]$ denotes the total fraction of states including Q_A^-, with the Q_B pocket either occupied or empty.

The stabilization of state $Q_AQ_B^-$ with respect to Q_A^-* reflected by K_2' is of crucial importance for the photosynthetic yield. Indeed, under steady-state illumination, the reaction center is half of the time in the "odd state" (i.e., with one electron residing either on Q_A or Q_B). A small value of K_2' would thus imply a large fraction of centers in the photochemically inactive Q_A^- state. An additional drawback would be to enhance back reactions. The stabilization of Q_B^- is essentially due to proton binding (*11*, *16*−*18*) either indirectly on neighboring protonatable groups (in chromatophores at pH ≥6 or in isolated reaction centers even at low pH) or by direct formation of neutral protonated semiquinone Q_BH (in chromatophores at low pH, see ref *19*). The value of K_2' has been estimated by various methods in isolated reaction centers of *R. sphaeroides*. The most accurate determinations are based on the comparison of the recombination rates for $P^+Q_A^-$ and $P^+Q_AQ_B^-$ (*11*, *12*, *20*, *21*) and on the damping of the semiquinone oscillation observed during a series of single turnover flashes (*22*). A very good agreement was obtained in both procedures, yielding $K_2' \approx 14$ at pH 8. When reaction centers are imbedded in their native membrane (chromatophores), the recombination rate of $P^+Q_AQ_B^-$ is slower than in isolated RCs (*5*, *6*, *19*, *23*, *24*) while that of $P^+Q_A^-$ is somewhat faster. This implies a larger value of K_2' in the native environment.

In the present work, we first compare the values of K_2' measured in chromatophores of *R. capsulatus* either based on recombination rates in the absence of a secondary donor or on the damping of the semiquinone oscillation in the presence of a secondary donor. The value of K_2' turned out to be about 5-fold larger in the absence of secondary donor than in its presence. This suggests an effect of P^+, which is present in the recombination experiments, but rapidly reduced in the oscillation experiments: P^+ appears to stabilize Q_B^- with respect to Q_A^-. In a second series of experiments, we further investigated the interactions between the donor and acceptor sides using a different approach. We determined the shifts in the reduction potential of the P^+/P couple caused by the presence of Q_B^- or Q_A^-. In contrast with the results on K_2', the latter experiments indicate that P^+ is stabilized more strongly by Q_A^- than by Q_B^-. The two sets of results can be reconciled by analyzing precisely the equilibria involved. This suggests that the energy of the $P^+Q_A^-$ state is markedly dependent on the type of occupation (distal or proximal) of the Q_B pocket.

MATERIALS AND METHODS

The mutant FJ2 of *Rhodobacter capsulatus* was a kind gift of Prof. F. Daldal (*25*). It is devoid of the physiological donors to the RC (cytochromes c_2 and c_y). A similar strain for *Rhodobacter sphaeroides*, CYC-17, was a kind gift of Prof. Donohue (*26*). This mutant lacks cytochrome c_2 and iso-c_2. Growth conditions and chromatophores preparation were previously described (*19*). Isolated reaction centers of *R. sphaeroides* R-26 were prepared according to ref *27*.

For spectroscopic experiments, the chromatophores were diluted in a medium containing 50 mM KCl and 50 mM Tris or MOPS buffer, pH 7.2. The RC concentration of the chromatophore suspension was around 100 nM, based on an extinction coefficient of 20 mM^{-1} cm^{-1} for P^+ at 600 nm. Valinomycin (3 μM) was added in order to collapse the membrane potential and associated absorption changes. In experiments using the exogenous donor TMPD (1 mM), the suspension was kept anaerobic under an argon flow.

Absorption changes were measured using a Joliot-type spectrophotometer, where the measuring light is provided by microsecond monochromatic flashes (*28*, *29*), as previously described (*19*). Actinic illumination was provided by a xenon flash (2 μs duration at half peak) filtered with a Schott RG-715 filter. The photodiodes used for detection were equipped with a Schott BG-39 filter for the visible range. In the near-IR a combination of high- and low-pass filters (CVI, LPF-650 and SPF-800), blocking bacteriochlorophyll fluorescence, was used. Due to low-frequency rejection by the electronics and also to the high peak intensity of the measuring flashes, actinic DC-light (as used in Figure 4) does not perturb the detection of absorption changes (even when it is not blocked by the filters placed on the photodiodes).

In the experiments of Figures 3 and 4, we measured the relative amounts of P^+, Q_A^-, and Q_B^- in the following manner. P^+ was measured at 603 nm (Figure 3, panels B and C) or 545 nm (Figure 4). From experiments on semiquinone oscillations using ferrocene as a donor, the contribution of Q_B^- at 603 nm was found isosbestic. On the other hand, by accumulating Q_A^- (using flashes or DC-light in the presence of ferrocene, ferrocyanide, and stigmatellin), a small contribution of Q_A^- was detected at 603 nm and the change was found isosbestic around 545 nm (see, however, footnote 3). This wavelength was retained as a pure P^+ indicator for experiments with stigmatellin. The extents of Q_A^- and Q_B^- were determined from absorption changes in the near-IR, due to electrochromic shifts of bacteriopheophytins (*24*, *30*, *31*). For Q_A^-, we used the change at 742 nm (close to the trough of the $Q_A^- - Q_A$ spectrum) and 755 nm for Q_B^- (peak of the spectrum).[2] These changes were corrected for the contribution of P^+, using the following ratios:

$$P^+(755\text{ nm}/603\text{ nm}) = 1.119 \quad (1)$$

$$P^+(742\text{ nm}/545\text{ nm}) = 0.524$$

These were determined from the spectrum of the reduction phase of P^+ observed in the presence of ferrocene. The relative amount of Q_B^-/RC was determined using the ratio

$$Q_B^-(\Delta A_{755\text{nm}}\text{ for 100\% RC})/$$
$$P^+(\Delta A_{603\text{nm}}\text{ for 100\% RC}) = 0.181 \quad (2)$$

[2] The wavelengths and calibration ratios given here are those for *R. capsulatus* chromatophores.

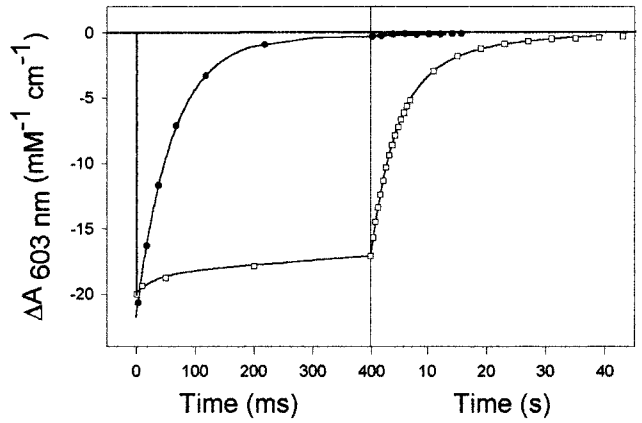

FIGURE 1: Decay of the flash-induced P^+ measured at 603 nm. Chromatophores of *R. capsulatus* FJ2, at pH 7.2, in the presence of 3 μM valinomycin (these conditions apply to all figures except panels C−D in Figure 3). Open squares, $P^+Q_B^-$ recombination with no inhibitor present. Solid circles, $P^+Q_A^-$ recombination with 40 μM stigmatellin. The solid curves are fits with parameters indicated in the text.

This calibration was obtained in the presence of TMPD. A small fraction of oxidized TMPD was present, allowing full reoxidation of Q_B^- in the dark period ($\geq$120 s) between experiments. A convenient check for this is the observation of a reduction phase of oxidized TMPD (monitored in the 100 ms range at 603 nm), which is correlated with the formation of quinol. The absence of this phase on the first flash after dark-adaptation is a sensitive test that no quinol is produced (i.e., that no Q_B^- was initially present). Under such condition, 100% Q_B^- is induced by the first flash.

For the calibration of the Q_A^- signal at 742 nm, two methods were used. The first one consists of subtracting the P^+ contribution from the $P^+Q_A^-$ change measured at 1 ms in the presence of stigmatellin. We obtained in this manner

$$Q_A^-(742\text{ nm})/P^+(545\text{ nm}) = 0.353 \quad (3)$$

A second method is to accumulate 100% Q_A^- by DC illumination in the presence of ferrocene, ferrocyanide, and stigmatellin (the 100% P^+ signal at 545 nm is obtained from a flash experiment). This yielded a value of 0.424 for the same ratio. The 20% difference between both methods reflects a real difference in the shape of the ($Q_A^- - Q_A$) spectrum in the IR (electrochromic) region, depending on the presence of P^+ (unpublished results). This was taken into account for estimating [Q_A^-] (used in eq A23, see Appendix) by solving the equation

$$(\Delta A_{742\text{nm}})/(\Delta A_{545\text{nm}} \text{ for 100\% } P^+) = 0.353[P^+Q_A^-] + 0.424[PQ_A^-] \quad (4)$$

where [PQ_A^-] was determined using eq A18. The unknown [$P^+Q_A^-$] is thus computed and one obtains [Q_A^-] = [$P^+Q_A^-$] + [PQ_A^-].

RESULTS

Estimation of K_2' from Recombination Kinetics. Figure 1 shows the time course of the absorption change induced by a short saturating flash at 603 nm, monitoring the oxidation and reduction of P in chromatophores of *R. capsulatus*-FJ2. This mutant is devoid of endogenous donors to P, so that the kinetics observed in the absence of inhibitor (open squares) reflect the $P^+Q_B^-$ recombination process, with $t_{1/2} \approx 3.15$ s. Also plotted in this figure (circles) is the trace observed in the presence of 40 μM stigmatellin, which is about 75-fold faster (from the ratio of the half-times). Stigmatellin is an efficient inhibitor of the Q_A^- to Q_B electron transfer, that binds to the Q_B pocket in a similar way as Q_B^- (*8*, *32*), and thus prevents UQ binding. The kinetics observed in the presence of this inhibitor reflect the recombination of $P^+Q_A^-$ with $t_{1/2} \approx 41$ ms (thus a rate constant $k_{PA} = 16.9$ s^{-1}). A minor slow phase (~2% in amplitude) is due to the release of the inhibitor and formation of Q_B^- in a small fraction of centers. This phenomenon is however much less pronounced with stigmatellin than with other inhibitors (*o*-phenantroline, terbutryn, or atrazine), as will be described in details in a forthcoming paper: we thus routinely used stigmatellin as the most efficient inhibitor of the Q_B pocket in chromatophores of *R. capsulatus*. Whereas the $P^+Q_A^-$ recombination kinetics are satisfactorily fitted by a single exponential, such is not the case for the decay of $P^+Q_B^-$, which is better adjusted by a sum of three exponentials (*19*). A small (2−10%, presently 7%) rapid component is generally present in the 100 ms range, presumably reflecting a $P^+Q_A^-$ recombination in a fraction of centers devoid of the secondary acceptor. The major phase (69%) has a $t_{1/2} \approx 2.8$ s, and a very slow phase ($t_{1/2} \approx 10$ s, 24% relative amplitude) is also present. The relative amplitude of this slow phase increases when submitting the system to multiple flashes or continuous illumination. This suggests an evolution of centers in the $P^+Q_B^-$ state toward a more stable conformation. In the following, we estimate the rate constant for $P^+Q_B^-$ recombination, k'_{PB} as that of the major phase, i.e., 0.25 s^{-1} [alternatively, one might derive k'_{PB} from the overall halftime, i.e., $\ln(2)/t_{1/2} = 0.22$ s^{-1}].

The decay of $P^+Q_B^-$ is due to the combination of two competing processes, namely the direct electron transfer from Q_B^- to P^+, with rate constant k_{PB} and the indirect route involving the $Q_AQ_B^- \leftrightarrow Q_A^-Q_B$ equilibrium and recombination from the $P^+Q_A^-$ state with an intrinsic rate constant k_{PA}. Thus, the observed rate constant should be

$$k'_{PB} = k_{PB} + k_{PA}\frac{1}{1 + K'_2} \quad (5)$$

As already mentioned, K'_2 is defined as

$$K'_2 = \frac{[Q_AQ_B^-]}{[Q_A^-*]} \quad (6)$$

where [Q_A^-*] denotes the sum of fractions of all possible Q_A^- states (i.e., with UQ absent or present on the Q_B site, either in the proximal or distal configuration). This is an "apparent" equilibrium constant which depends on the binding equilibrium of UQ at the Q_B site.

In isolated reaction centers where the recombination of $P^+Q_B^-$ is faster than in chromatophores, by a factor of 3−5 (*5*, *6*, *19*, *23*, *24*), the indirect pathway dominates and the direct recombination rate (k_{PB} in eq 1) is believed to be almost negligible while this is not quite so in chromatophores. For instance, in isolated RCs from *R. sphaeroides* the decay of

$P^+Q_B^-$ has a $t_{1/2}$ of about 1 s (i.e., $k'_{PB} \approx 0.7\ s^{-1}$) at pH 7 (*11*), while k_{PB} has been estimated $\leq 0.1\ s^{-1}$ (*11*), in agreement with the value of 0.06 s^{-1} found in mutant RCs (*12*). Larger values were, however, measured in wild-type RCs with modified Q_A, i.e., 0.12 s^{-1} (*14*) and 0.19 s^{-1} (*15*). In isolated RCs from *R. capsulatus*, k_{PB} can be estimated to be about 0.08 s^{-1} from the limiting rate observed at pH 4 (*33*), while k'_{PB} is around 0.65 s^{-1} at pH 7 (*34*). In *R. capsulatus* chromatophores we obtained the same value $k_{PB} \approx 0.08\ s^{-1}$ from the limiting value observed at pH ≤ 6 (*19*). Therefore, this should be subtracted from the observed value of k'_{PB} to estimate the second term of eq 5, i.e.,

$$k_{PA}\frac{1}{1+K'_2} = 0.17\ s^{-1} \quad (7)$$

Using the value of $k_{PA} = 16.9\ s^{-1}$, one obtains

$$K'_2(P^+) = 98 \quad (8)$$

(this notation is meant to indicate that the equilibrium was measured in the presence of P^+).

Estimation of K'_2 from the Damping of Semiquinone Oscillations. When the reaction centers are subjected to a series of single turnover flashes in the presence of an efficient electron donor to P^+, Q_B^- is formed on odd-numbered flashes and destroyed on even-numbered flashes. This period-2 oscillation is damped due to the fraction of centers in the Q_A^- state in equilibrium with $Q_AQ_B^-$. These centers are photochemically inactive and cause a phase retardation. Thus, the damping of the oscillation provides a means to estimate K'_2 (*22*). The equilibrium constant measured in this manner relates to centers where P is in the reduced state and will be noted K'_2(P).

Figure 2 (top panel) shows the semiquinone oscillations measured at 755 nm in the presence of reduced TMPD, ensuring total P^+ reduction with $t_{1/2} \approx 1$ ms. The top curve shows the slow semiquinone decay due to oxidized TMPD observed after a single flash, that was used to estimate the semiquinone loss occurring between consecutive flashes. The bottom panel is a plot of the absolute values of the change induced by each flash. K'_2(P) is determined from the exponential fit of these data, using eqs A4−5, and corrected for the semiquinone leak using eq A2. From several such experiments (estimating the error bar from the scatter), we obtained

$$K'_2(P) = 21 \pm 2 \quad (9)$$

This method relies on the assumption that the acceptor side equilibrium is the sole cause of damping. In general, damping may be caused by photochemical "misses" or "double-hits". *Misses* can be due to three factors: rapid back-reactions, lack of saturation, or reoxidation of semiquinone during the time interval between consecutive flashes. Back-reactions may occur at the P^+Bphe^- stage, but the lifetime of this state is very short, so that a saturating microsecond flash takes care of this problem by allowing multiple turnovers for RCs that have back-reacted in this manner. Recombination from $P^+Q_A^-$ is minimized due to the short lifetime of Q_A^- ($t_{1/2} \approx 70\ \mu s$ at pH 7.2, compared with $t_{1/2} \approx 40$ ms for the recombination reaction) and so is the recombination from $P^+Q_B^-$ ($t_{1/2} \approx 3$ s) because of the 1 ms reduction of P^+ by

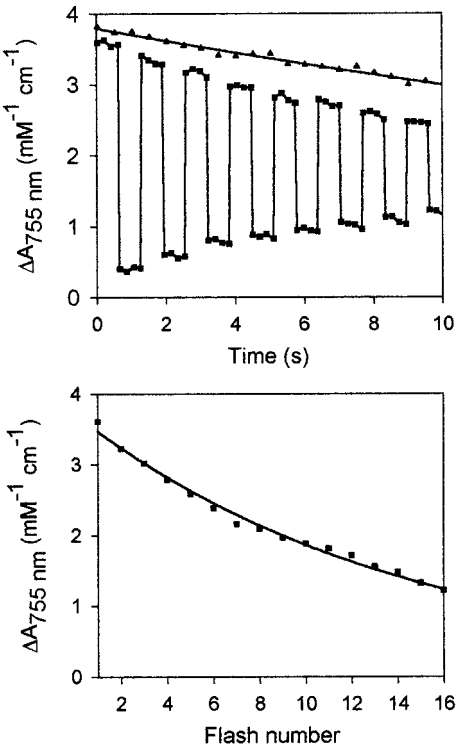

FIGURE 2: (Top panel) Q_B^- oscillations measured at 755 nm during a series of saturating flashes (spaced 640 ms apart) in the presence of 1 mM TMPD. The top trace is the decay of Q_B^- after a single flash, used to correct the damping for the 1.6% decay occurring between two successive flahes, according to eq A2. The initial extent of Q_B^- is larger than in the multiple flash experiment because a small fraction of centers with Q_B^- was initially present in the latter. Bottom panel, a plot of the successive changes caused by each flash relative to the previous flash (with sign inverted on even numbered flashes) and (line) the fit with an exponential decay (see eqs A4 and A5). The corrected value obtained for K'_2 in this particular experiment was 19 (the uncorrected value was 14.5).

TMPD. Reoxidation of Q_B^- between successive flashes was estimated as described above. Care was taken to check that the flashes were fully saturating (e.g., doubling the flash energy did not affect the oscillations monitored on a long flash series). *Double-hits* may occur when the flash duration is insufficiently short with respect to RC turnover. Such is not the case here (2 μs flash width vs 1 ms lifetime of P^+). Another cause of double-hits may be an actinic effect of the measuring beam that would induce a phase advance. We checked that the actinic effect of the detecting flashes was negligible: decreasing by a factor of 3 the energy of the measuring light had no effect on the oscillations or on the decay rate of Q_B^- after a single flash.

The value of K'_2(P) is 4.7-fold smaller than $K'_2(P^+)$ estimated from recombination kinetics (eq 8). This suggests that the presence of P^+ might somehow stabilize Q_B^- relative to Q_A^-, accounting for an increase of K'_2. If such is the case, one may expect a reciprocal effect of the state of the acceptor side on the midpoint potential of the P^+/P couple.

Shifts of the Midpoint Potential of P^+/P in the Presence of Q_B^- or Q_A^-. The rationale of the following experiments is to poise the ambient redox potential in a region where P^+ is titrated and to monitor the change in the amount of P^+ caused by the presence of Q_B^- or Q_A^-. We used ferri- and ferrocyanide as a redox buffer and ferrocene as a mediator

ensuring relatively rapid equilibrium with P. We first discuss the interactions of these substances with the RC.

When 800 μM ferrocyanide was added alone (not shown), only a slight acceleration of the P^+ decay was observed (with respect to the recombination of $P^+Q_B^-$), showing that the reduction of P^+ by this substance is a slow process. On the other hand, when adding, e.g., 150 μM ferrocene alone (Figure 3A, solid circles), a major phase of P^+ reduction occurred with $t_{1/2} = 18$ ms followed by a slow phase ($t_{1/2} =$ 220 ms, 17%). From experiments monitoring the decay of the membrane potential from the carotenoid bandshift (not shown), we have concluded that this slow phase corresponds to the flow of oxidized ferrocene (ferricinium) from the inner space of the chromatophore, i.e., to a relaxation of the transient high redox potential due to local accumulation of this oxidant within the vesicle. As can be seen in Figure 3A, the slow phase is suppressed on the second flash (but can be restored by adding inhibitors of the cytochrome *b*-c_1 complex, such as myxothiazol). This is due to rapid reduction of ferricinium inside the vesicle by the *b*-c_1 complex, which takes place when quinol is released from the RC after the second flash (thus ferrocene acts as a substitute to cytochrome c_2, both on the RC and *b*-c_1). When the slow phase is completed, i.e., at times longer than, say, 1 s, P is fully equilibrated with the ferrocene present in the bulk medium. Finally, we note that ferrocene reacts readily with ferrocyanide (*17*).

Figure 3B shows the flash induced kinetics monitoring P^+ at 603 nm (solid circles) or Q_B^- at 755 nm (open circles, corrected from the contribution of P^+) in the presence of ferrocyanide (800 μM) and ferricyanide (2 mM). The decreased amount of flash-induced P^+ corresponds to the partial oxidation of P in the dark at the potential imposed by our redox mixture. The fraction of P^+ present in the dark is $w = 0.23$. The slow decay of Q_B^- observed under such conditions shows that there is no rapid equilibration of the acceptor side with the redox buffer. A slow phase of P^+ decay is now present with the same kinetics as that of Q_B^-. This feature occurs at times much longer than the redox equilibration of P and indicates a downward shift of its E_m caused by the interaction with Q_B^-. The constant ratio of ΔP^+ (excess P^+ with respect to the dark adapted state) over $[Q_B^-]$ was $y = 0.096$ (using calibrations described in the Materials and Methods). Then, using eq A13, one obtains $\Delta E_{m,P}(Q_B^-) = -11 \pm 3$ mV (here and below, the accuracy range was estimated by taking into account the scatter of results in three to five experiments and the error estimated in a similar way for the calibration figures).

The same method was applied to isolated reaction centers from *R. sphaeroides* R-26, reconstituted with UQ-6. Figure 3C shows the results of such an experiment, yielding $\Delta E_{m,P}(Q_B^-) = -10 \pm 3$ mV. We also used this approach to determine the $\Delta E_{m,P}$ caused by Q_A^- (Figure 3D) in this material (with no secondary quinone added and 20 μM stigmatellin present). A high concentration of ferrocene (800 μM) had to be used to ensure a rapid redox equilibration of P ($t_{1/2} \approx 2$ ms) with respect to recombination ($t_{1/2} \approx 60$ ms). The value of $\Delta E_{m,P}(Q_A^-)$ thus obtained was -18 ± 3 mV.

We had to resort to a different method for measuring $\Delta E_{m,P}(Q_A^-)$ in chromatophores, because we could not achieve a sufficiently rapid redox equilibration of the donor with respect to the lifetime of the flash-induced Q_A^-. In FJ2

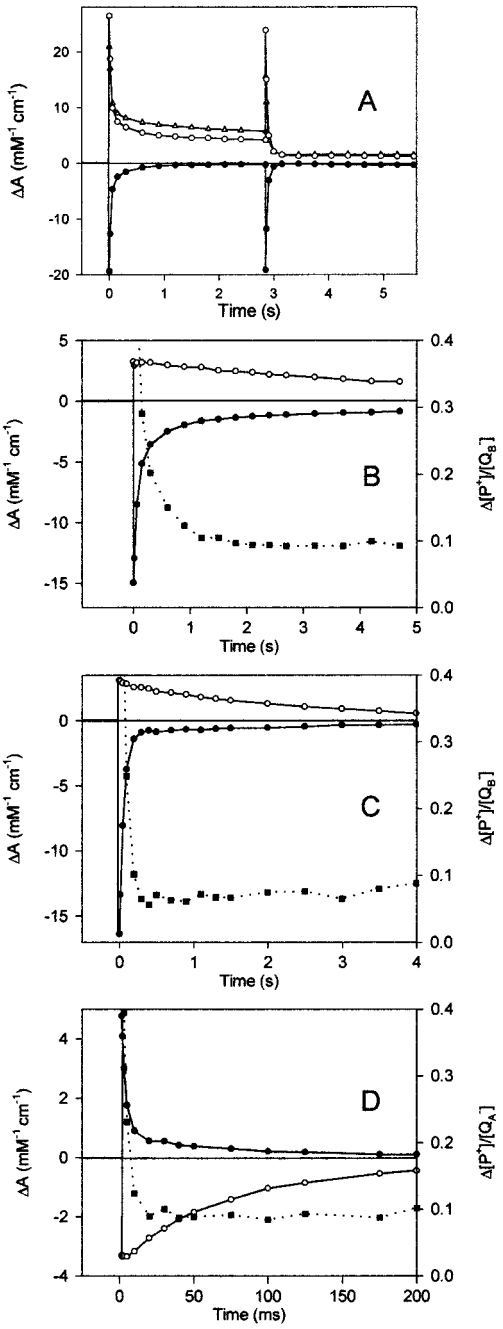

FIGURE 3: (A) Absorption changes caused by two saturating flashes (spaced 2.85 s apart) in the presence of 150 μM ferrocene. Solid circles, 603 nm. Open triangles, 450 nm. Open circles, 755 nm. The 603 nm change essentially monitors P^+, while the 450 and 755 nm changes monitor both P^+ and Q_B^-. (B) Absorption changes at 603 nm (solid circles) and 755 nm (open circles) following a saturating flash in the presence of 150 μM ferrocene, 800 μM potassium ferrocyanide, and 2 mM potassium ferricyanide. The 755 nm trace was corrected for the P^+ contribution (see Materials and Methods). The solid squares show the ratio of $\Delta P^+/[Q_B^-]$ (reaching a constant value $y \approx 0.096$ after 1 s), plotted against the right-hand scale. (C) Same experiment as in panel B, but with 0.47 μM isolated reaction centers from *R. sphaeroides* R-26, in the presence of 15 μM UQ-6, 50 μM ferrocene, 800 μM ferrocyanide, and 8 mM ferricyanide. Solid circles, 603 nm change. Open circles, 758 nm change corrected for the P^+ contribution. Solid squares, $\Delta P^+/[Q_B^-]$ (right-hand scale). (D) R-26 isolated reaction centers with no added quinone and 20 μM stigmatellin, 800 μM ferrocene, 800 μM ferrocyanide, and 8 mM ferricyanide. Solid circles, 550 nm change (monitoring P^+). Open circles, 750 nm change (monitoring Q_A^-, corrected for the P^+ contribution). Solid squares, $\Delta P^+/[Q_A^-]$ ratio (right-hand scale).

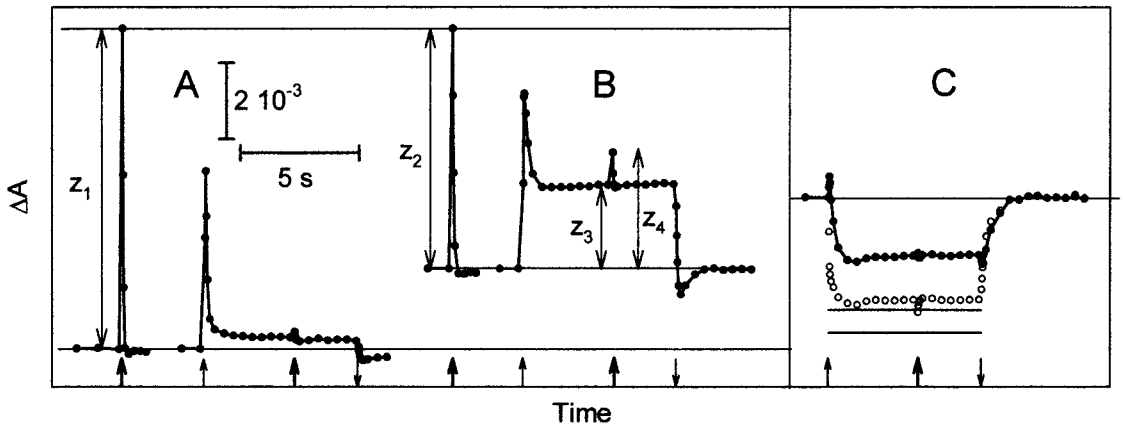

FIGURE 4: (A) Absorption changes monitoring P^+ at 545 nm following a saturating flash (left-hand trace), or during a continuous illumination to which a saturating flash was superimposed (right-hand trace). The bold arrows at the bottom indicate flash triggering and thin arrows indicate shutter opening (pointing up) and closure (pointing down). Ferrocene (100 μM), ferrocyanide (800 μM), and stigmatellin (50 μM) were present. (B) Same as panel A, except 1.6 mM ferricyanide was added. The plots of panel B were offset so that the flash-induced P^+ reaches the same level as in panel A (thus the baseline indicates the amount of P^+ present in the dark). (C) Solid circles, 742 nm change recorded under the same conditions as the right-hand trace of panel B. The open circles show the Q_A^- change after correcting the 742 nm trace from the P^+ contribution. The horizontal lines indicate the 742 nm level expected for 100% Q_A^- in the presence of P (bottom line) or P^+ (upper line).

chromatophores, the reduction rate of P^+ by ferrocene saturates above 150 μM ferrocene, with $t_{1/2} \approx 20$ ms but the major problem is the 200 ms phase due to the slow outflow of ferricinium. The procedure illustrated in Figure 4 is based on the steady-state equilibria under a continuous illumination analyzed in the Appendix. The same type of redox buffering as above was used (ferro/ferricyanide + ferrocene) and its effect on P^+/P in the dark was measured by comparing the flash-induced P^+ signal (z_2) with that (z_1) obtained under reducing conditions. Due to the presence of the inhibitor (stigmatellin), there is no (or little, see below) net electron flow in the system under steady-state illumination, so that if $E_{m,P}$ were constant, the $[P^+]/[P]$ ratio at steady-state would be imposed by the redox poise independently of the amount of accumulated Q_A^-. Thus, the absorption change monitoring P^+ should return to the dark baseline after some transient. Conversely, if the centers possessing Q_A^- have a different $E_{m,P}$, one should have a nonzero steady-state level of P^+ with respect to the baseline. This was indeed observed (level noted z_3 in panel B).[3] To quantify the effect, we need information on the amount of Q_A^- sustained during the illumination. This can be obtained in two ways. A first method (1) is to monitor the extent of P^+ induced by a flash superimposed on the continuous illumination (level z_4). Since only centers in the PQ_A state are photochemically active, their relative amount is the difference $(z_4 - z_3)/z_1$, while the fraction of PQ_A^- centers is $(z_2 - z_4)/z_1$. Equation A22 expresses $\Delta E_{m,P}$ as a function of the four z levels. The second method (2) consists of measuring the steady-state level of Q_A^- at an appropriate wavelength. This was done at 742 nm (Figure 4C), which is close to the trough of the Q_A^- spectrum, is isosbestic for Q_B^- and where the contribution of P^+ is relatively small. The latter was corrected using the figures given in Materials and Methods. The fraction $[Q_A^-]$ was then inserted in eq A23, yielding a second estimate for $\Delta E_{m,P}$. The values thus obtained for $\Delta E_{m,P}(Q_A^-)$ were −33 and −31 mV, using methods 1 and 2, respectively. As argued in the Appendix, the agreement between both methods is a sensitive test that validates the assumptions made in this treatment (especially that of a negligible leak through the stigmatellin block). Under proper conditions (short duration of the experiment, keeping the ferri/ferrocyanide ratio below 2.5), we consistently obtained values of $\Delta E_{m,P}$ in the range −35 to −30 mV (using both methods 1 and 2), varying the ferrocene concentration (50−200 μM range), the ferri/ferrocyanide concentrations, and the illumination intensity (by a factor of 4). On the basis of these results (and taking into account the trend toward an overestimation of $\Delta E_{m,P}$, see Appendix) we estimate $\Delta E_{m,P}(Q_A^-) = -30 \pm 5$ mV.

DISCUSSION

We have presented a series of results pertaining to the electron-transfer equilibrium between the primary and secondary quinone acceptors in chromatophores of *R. capsulatus*. From recombination kinetics, we estimate $K_2' \approx 100$. From the damping of semiquinone oscillations in the presence of an electron donor to P^+, we obtain $K_2' \approx 21$ (25 in *R. sphaeroides*). A noteworthy difference between the conditions of these measurements is the state of the primary donor, which is oxidized in the first case and reduced in the second one. We therefore looked for a differential interaction of P^+ with Q_A^- and Q_B^- which could account for the ~5-fold increase of K_2' observed in the presence of P^+. We did find a differential interaction from the shifts of the midpoint potential of P induced by Q_A^- or Q_B^-, but in the opposite

[3] The negative overshoot of P^+ observed (panel B) when shutting the light off is well explained on the following grounds. During the illumination there is an excess of accumulated Q_A^- with respect to P^+. When the light is shut off, these electrons are reinjected toward the donor side through recombination. This causes a transient excess of reduced ferrocene (and lower E_h than the bulk medium) inside the vesicles that relaxes at a rate limited by ferricinium reentry. A small negative overshoot is also present in the experiment of panel A (reducing conditions). In this case, the return (rise) to the baseline is much slower, as expected for a Q_A^- contribution under reducing conditions, suggesting that in this experiment 545 nm is not strictly isosbestic for this change (we observed some fluctuations, from 543.5 to 545 nm, when determining the isosbestic wavelength for Q_A^-). Due to its small size, this contamination by Q_A^- is of no significant consequence in the estimate of the $\Delta E_{m,P}$.

direction: $\Delta E_{m,P}$ (Q_B^-) ≈ -11 mV and $\Delta E_{m,P}$ (Q_A^-) ≈ -30 mV. Therefore, P^+ stabilizes both Q_A^- and Q_B^-, but the larger effect on the former would apparently predict a 2-fold *decrease* of K_2' in the presence of P^+. Before scrutinizing the information really contained in the whole set of results, we first examine some particular aspects.

The estimate of K_2' based on recombination rates relies on several assumptions. One of these is that the rate k_{PA} observed in the presence of an inhibitor is representative of its value in the absence of inhibitor. Several arguments support this view. First, the value of k_{PA} is the same (or almost so) for all the inhibitors we tested (stigmatellin, atrazine, terbutryn, and *o*-phenantroline) despite very different dissociation constants and rates (Ginet and Lavergne, forthcoming paper). Second, in isolated reaction centers, the same k_{PA} is observed whether the Q_B pocket is empty or occupied by an inhibitor. A second assumption used in our estimate of K_2' was to subtract the rate constant for direct recombination, $k_{PB} = 0.08\ s^{-1}$ that we estimated previously (*19*). If this value happens to be overestimated, one still would have $K_2' \geq 67$.

The values that we obtained for the shift of the reduction potential of P caused by Q_A^- or Q_B^- may be explained on the grounds of simple Coulombic interactions (but, as discussed below, the effect involving Q_A^- cannot be simply separated from the energetics of stigmatellin binding). The center to center distance between P^+ and Q_A^- is about 28 Å. The appropriate value of the dielectric constant ϵ is a matter of debate. A value of 4 was assigned to the protein interior (*35*) taking into account electron polarization and some rearrangement of protein dipoles. For unclear reasons, calculations using a higher value ($\epsilon \approx 20$) give a better agreement with experimental pK_as (*36*, *37*). It may be expected that the inner core of the protein has a low dielectric constant like $\epsilon \approx 4$ while the value $\epsilon \approx 20$ is appropriate for more peripheral regions (*38*) so that the relevant ϵ in our case should be intermediate between these values. An elementary dipole over a 28 Å distance would give an interaction energy of 128 meV for $\epsilon = 4$ and 26 meV for $\epsilon = 20$. The electrostatic interaction must however be somewhat decreased due to the fractional proton release caused by P^+ and fractional proton uptake caused by Q_A^- (*16*, *17*). The smaller interaction with Q_B^- (~ -11 mV) could be accounted by the larger proton uptake and the more polar character of the Q_B region. In our chromatophores, we estimated the proton uptake by $Q_B^- \approx 0.9-1$ at pH 7.2 (*19*) and (data not shown) 0.26−0.3 for Q_A^-. In isolated reaction centers from *R. sphaeroides* R-26, we obtained $\Delta E_{m,P}(Q_A) \approx -18$ mV and $\Delta E_{m,P}(Q_B) \approx -10$ mV. The smaller interaction with Q_A^- may reflect an increased ϵ of the solubilized RC with respect to chromatophores. On the other hand, the finding of very similar values for $\Delta E_{m,P}(Q_B)$, may be due to the larger proton uptake in chromatophores compared with isolated reaction centers [estimated in R-26 about 0.4 H^+/Q_B^- (*16*) or 0.8 (*17*)] which can compensate the effect of ϵ. In their work on proton uptake and release in the various charged states of R-26 reaction centers, McPherson and co-workers (*16*) found no significant difference for the net uptake in the presence of $P^+Q_A^-$ compared with the summed effects of P^+Q_A and PQ_A^-. This result may not be incompatible with ours, since the interaction of 18 mV that we find in this material would imply pK shifts of 0.3 units, which is probably below the experimental accuracy of the proton uptake titrations.

We will now examine more precisely the information contained in our data and see how they can be combined. On one hand, we have the effect of the state of P on K_2':

$$K_2'(P) = \frac{[PQ_AQ_B^-]}{[PQ_A^-*]} \approx 21 \tag{10}$$

$$K_2'(P^+) = \frac{[P^+Q_AQ_B^-]}{[P^+Q_A^-*]} \approx 98 \tag{11}$$

The ratio of these expressions is

$$\frac{[P^+Q_AQ_B^-][PQ_A^-*]}{[P^+Q_A^-*][PQ_AQ_B^-]} \approx 4.7 \tag{12}$$

This can be expressed as a shift of the midpoint potential of P depending on the state of the acceptors:

$$E_{m,P}(Q_A^-*) - E_{m,P}(Q_AQ_B^-) = 58 \log\left[\frac{[P^+Q_AQ_B^-][PQ_A^-*]}{[PQ_AQ_B^-][P^+Q_A^-*]}\right] \approx 39\ \text{mV} \tag{13}$$

On the other hand, we measured the ΔE_m of the P^+/P couple induced by the presence of Q_B^-, which is

$$E_{m,P}(Q_B^-) = 58 \log\left[\frac{[P^+Q_A*][PQ_AQ_B^-]}{[PQ_A*][P^+Q_AQ_B^-]}\right] \approx -11\ \text{mV} \tag{14}$$

and that due to Q_A^-:

$$E_{m,P}(Q_AS^-) = 58 \log\left[\frac{[P^+Q_AS][PQ_A^-S]}{[PQ_AS][P^+Q_A^-S]}\right] \approx -30\ \text{mV} \tag{15}$$

where S indicates that stigmatellin was bound to the Q_B pocket.

To connect the information contained in eqs 13−15, we need an estimate of the possible shift of $E_{m,P}$ caused by stigmatellin binding, i.e., $E_{m,P}(Q_A*) - E_{m,P}(Q_AS)$. This is easily done by determining the midpoint potential of P in the absence or presence of stigmatellin. We measured the flash-induced amount of P^+ over a range of ferri/ferrocyanide under both conditions and obtained the plots of Figure 5, showing that $E_{m,P}$ is independent of the presence of stigmatellin within a few millivolts. A similar result was obtained with the inhibitor terbutryn.

Figure 6 summarizes the effects on $E_{m,P}$ of the various states of the acceptor side. The values of $E_{m,P}(Q_AT)$ and $E_{m,P}(Q_A^-T)$ in the presence of another inhibitor, terbutryn, are also featured in Figure 6. $E_{m,P}(Q_AT)$ was obtained from the titration of Figure 5. The value of $E_{m,P}(Q_A^-T)$ was derived from measurements (data to be published in a forthcoming paper) of the apparent dissociation constant of terbutryn, (K_T') in the presence of PQ_A^- and $P^+Q_A^-$. This dissociation constant was little affected by the state of P, with $K_T'(PQ_A^-) \approx 26\ \mu$M and $K_T'(P^+Q_A^-) \approx 22\ \mu$M [whereas it was markedly

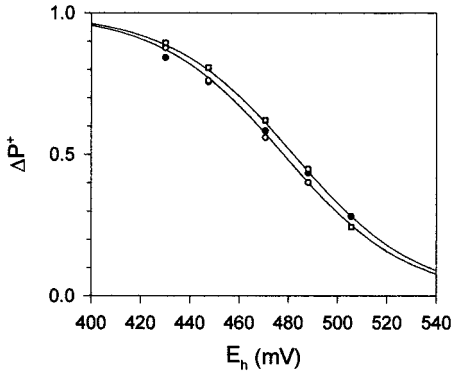

FIGURE 5: Redox titration of P, with no inhibitor (solid circles), 25 μM stigmatellin (open circles), or 100 μM terbutryn (open squares). The vertical scale is the relative extent of the flash-induced change at 603 nm. The potential was varied by adding ferricyanide in the presence of 400 μM ferrocyanide and the horizontal scale was computed as $E_h = 430$ mV + 58 log[ferri]/[ferro]. Identical results were obtained when running the titration in the reductive direction. The solid lines are best fits of the data with one-electron Nernst curves, yielding $E_{m,P} = 478$ mV (no inhibitor or stigmatellin) and 482 mV (terbutryn).

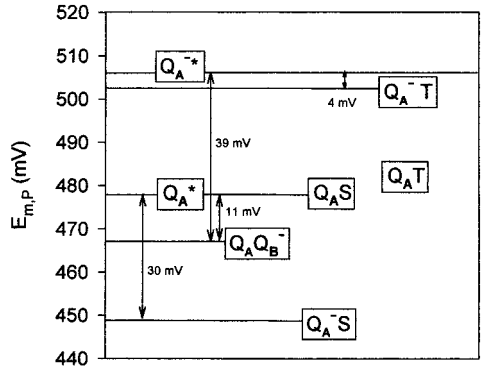

FIGURE 6: A diagram showing the midpoint potential of the P^+/P couple, depending on the state of the acceptor side. $E_{m,P}$ (Q_A*), $E_{m,P}$ (Q_AS), and $E_{m,P}$ (Q_AT) are obtained from the experiment of Figure 5. $E_{m,P}$ ($Q_AQ_B^-$) and $E_{m,P}$ (Q_A^-S) are located with respect to the former level, using $\Delta E_{m,P}(Q_B^-) \approx -11$ mV (from experiments such as that of Figure 3B) and $\Delta E_{m,P}(Q_A^-) \approx -30$ mV (from experiments such as that of Figure 4). The level of $E_{m,P}$ (Q_A^-*) is positioned with respect to $E_{m,P}$ ($Q_AQ_B^-$) using the ratio $K_2'(P^+)/K_2'(P)$ and eq 13.The level of $E_{m,P}$ (Q_A^-T) is placed 4 mV below $E_{m,P}$ (Q_A^-*) using unpublished data for the apparent dissociation constant of terbutryn in the presence of PQ_A^- and $P^+Q_A^-$ (see text).

affected by the state of Q_A: $K_T'(PQ_A) \approx 6$ μM]. These data locate $E_{m,P}(Q_A^-T)$ about 4 mV below $E_{m,P}(Q_A^-$*).

We also found a difference between $K_2'(P)$ and $K_2'(P^+)$ in chromatophores of *R. sphaeroides* (CYC-17), but with a much smaller extent than in *R. capsulatus*. In *R. sphaeroides* (at pH 7.15), we obtained $k_{PA} = 14.4$ s^{-1} for the $P^+Q_A^-$ recombination, satisfactorily adjusted by a single exponential. The decay of $P^+Q_B^-$ was biexponential with half-times of 540 ms (25%) and 2.5 s (75%). Thus, one has $K_2'(P^+) = 33$, based on the overall $t_{1/2}$ of the recombination of $P^+Q_B^-$, or 51, based on the rate of the major exponential phase. On the other hand, from the damping of semiquinone oscillations, we obtained $K_2'(P) = 25$. We could not determine $\Delta E_{m,P}$ in the presence of Q_A^- or Q_B^- in this material because the ferrocene-mediated equilibration of P is too slow (the slow phase discussed about Figure 3A and ascribed to transient accumulation of ferricinium in the internal space is both larger and slower in these chromatophores).

In isolated reaction centers from *R. sphaeroides*, very similar values for $K_2'(P)$ and $K_2'(P^+)$ (∼14) were reported (*11*, *22*). This difference between isolated reaction centers and chromatophores may be due to modified properties of the Q_B pocket (see ref *19*) and also, possibly, to the different modalities for the interaction with the UQ pool [a RC-detergent micelle contains a small discrete number of UQ molecules, slowly exchanging with quinone-detergent micelles (*39*)]. Indeed, in the latter paper, Shinkarev and Wraight estimated $K_2'(P^+) \approx 22$ when correcting for the effect of UQ distribution among micelles. As noted by these authors, this effect is probably suppressed when using the more water-soluble UQ-0, as was done in the measurement of $K_2'(P)$ from semiquinone oscillation in ref *22*. An additional cause for underestimation of $K_2'(P^+)$ in (*11*) is that more recent data show that the direct route for $P^+Q_B^-$ recombination is not really negligible [i.e., $k_{BP} = 0.12-0.19$ s^{-1} (*14*, *15*)]. This would entail $K_2'(P^+) \approx 18-19$ (at pH 8). If the corrrection suggested by Shinkarev and Wraight is further applied, $K_2'(P^+)$ may be as high as 28. Therefore, in this material, the $E_{m,P}(Q_A^-$*) level would be located about 7 mV (k_{PB} correction) or 18 mV (k_{PB} and Shinkarev's corrections) above that of $E_{m,P}(Q_AQ_B^-)$, whereas we found an opposite difference of $10-18 = -8$ mV between $E_{m,P}(Q_A^-S)$ and $E_{m,P}(Q_AQ_B^-)$. Thus, the effects found in *capsulatus* chromatophores may be present in isolated RCs from *sphaeroides* although to a smaller extent, i.e., 15−26 mV instead of 60 mV for the gap between $E_{m,P}(Q_A^-$*) and $E_{m,P}(Q_A^-S)$.

A conservative conclusion of the present results is that the donor and acceptor side of the reaction center in chromatophores interact in a complex manner, which cannot be entirely due to electrostatics.[4] Our data, as summarized in Figure 6, give no direct information on the energy of individual states of the reaction center (such as PQ_A*, P^+Q_A*, etc.), but rather on energy differences between pairs of such states (but see below). The most dramatic effect is a ∼60 mV shift between $E_{m,P}(Q_A$-S) and $E_{m,P}(Q_A^-$*) [or $E_{m,P}(Q_A^-T)$]. This indicates that the apparent dissociation constant of stigmatellin is about 10-fold larger for state PQ_A^- compared with state $P^+Q_A^-$. The data could also be expressed in terms of $E_{m,QA}$ (i.e., the midpoint potential of Q_A). Indeed, we have relations such as

$$E_{m,P}(Q_AX) - E_{m,P}(Q_A^-X) = E_{m,QA}(P^+X) - E_{m,QA}(PX) \quad (16)$$

where X denotes some state of the Q_B pocket. It follows that when oxidizing P, the midpoint potential of Q_A is decreased by about 28 mV in the absence of inhibitor, but raised by about 30 mV in the presence of stigmatellin.

We can, however, gain more insight by making additional assumptions on the purely electrostatic contribution to the network of interactions pictured in Figure 6. As a first approximation we may for instance assume that, as suggested above, the shifts of $E_{m,P}$ caused by Q_A^-S (−30 mV) and Q_B^- (−10 mV) essentially reflect the Coulombic energy between the charged donor and acceptors. This would imply

[4] An independent piece of information is the difference, mentioned in section Methods, between the ($P^+Q_A^-S - PQ_AS$) spectrum in the IR region and the sum of spectra ($P^+ - P$) and ($PQ_A^-S - PQ_AS$). For instance, the ($Q_A^-S - Q_AS$) change is positive at 758 nm in the absence of P^+ and negative in the presence of P^+ (unpublished results).

that, in the diagram of Figure 6, the location of all states except Q_A^-* and Q_A^-T can be at least roughly accounted for by the sole electrostatic interactions and that the energies of states with UQ, S, or T bound to the Q_B pocket in the presence of oxidized Q_A are little affected by the state of P. Conversely, the anomalous locations of $E_{m,P}(Q_A^-*)$ and $E_{m,P}(Q_A^-T)$ mean that the energy of states $P^+Q_A^-$* or $P^+Q_A^-T$ is markedly increased for some "conformational" reason. Compared with states where either P is reduced or Q_A oxidized, this increase is by about 60 mV, taking into account the assumed 30 mV electrostatic stabilization of the $P^+Q_A^-$ state. Let us examine in more detail the various relevant states of the Q_B pocket. The collective state denoted with a star covers an equilibrium between three substates where the Q_B pocket is either empty or occupied with distal or proximal UQ. In the presence of the large UQ pool of chromatophores, the pocket is probably occupied most of the time and, according to some current views (*7*, *8*), the oxidized quinone is mostly bound at the distal site. Thus, the "star" state would essentially reflect UQ bound at the distal position. On the other hand, crystallographic studies have established that stigmatellin binds at the proximal site (*8*, *32*) whereas terbutryn (*40*) (see also ref *32* for atrazine) binds at a more distal position, overlapping the distal and proximal UQ sites. We thus propose that the $P^+Q_A^-$ state specifically entails a conformational constraint when the distal site is occupied and that this constraint is released when the proximal site is occupied by stigmatellin. The above analysis relies on the assumption that the values of $\Delta E_{m,P}$ found for $Q_AQ_B^-$ and Q_A^-S are essentially due to electrostatics, so that we can assign conformational effects specifically to state Q_A^-* (or Q_A^-T). It would, however, remain qualitatively valid as long as the electrostatic contributions are not drastically different from our estimates.

Our data give no clue as to the molecular mechanism which is responsible for destabilizing the $P^+Q_A^-$* state. Interestingly, in chloroplast Photosystem II, Krieger and Rutherford (*41*−*43*) have reported an interaction between the donor side (O_2-evolving system) and the acceptor side. Concerning functional aspects, we notice that increasing $K_2'(P^+)$ is advantageous to photosynthesis because this decreases recombination. This could be done by increasing the stabilization of Q_B^- irrespective of the state of P, but there is a limit to that, because increasing the midpoint potential of the Q_B/Q_B^- couple entails lowering that of Q_B^-/QH_2 and will decrease the driving force for the second electron transfer. On the other hand, increasing K_2' specifically in the presence of P^+ is entirely beneficial, because this is a photochemically closed state where the second electron-transfer cannot occur. According to our analysis, the increase of $K_2'(P^+)$ is essentially obtained by destabilizing the state $P^+Q_A^-$*. An additional consequence, if the stabilization observed with stigmatellin also occurs for UQ binding at the proximal site, will be to lower the energetic barrier for quinone rearrangement which is believed to be the rate-limiting step for electron transfer on the acceptor side (*7*). Similarly, on the donor side, the increased potential of P in the presence of Q_A^- will facilitate the reduction of P^+, which may be advantageous to limit recombination when the UQ pool is substantially reduced.

ACKNOWLEDGMENT

We wish to thank A. Verméglio for helpful discussions and reading the mansucript. The gifts of strain FJ-2 by Prof. F. Daldal and of CYC-17 by Prof. T. Donohue are gratefully acknowledged.

APPENDIX

Oscillation Damping. If y_n denotes the amount of semiquinone ($Q_A^- + Q_B^-$) present after flash n, the fraction of centers in state Q_A^- is $y_n/(1 + K_2')$. Hence the recurrence law:

$$y_{n+1} = T - y_n \frac{K_2'}{1 + K_2'} \tag{A1}$$

where T stands for the total amount of RC. In the case when a fraction α of the semiquinone is reoxidized during the flash interval, this expression becomes

$$y_{n+1} = T - y_n \frac{(1 - \alpha)K_2'}{1 + K_2'} \tag{A2}$$

A convenient method for determining the damping is to plot the absolute values of the successive differences $|\Delta_n| = |y_{n+1} - y_n|$. From eq A1, one derives the recurrence law:

$$|\Delta_{n+1}| = |\Delta_n| \frac{K_2'}{1 + K_2'} \tag{A3}$$

Therefore:

$$|\Delta_n| = |\Delta_0| \exp(-kn) \tag{A4}$$

with

$$K_2' = \frac{e^{-k}}{1 - e^{-k}} \tag{A5}$$

Determination of $\Delta E_{m,P}$ in the Presence of Q_B^-. We note E the ambient redox potential, E_m the midpoint potential of the P^+/P couple, and w the fraction of centers in state P^+ in the absence of Q_B^-. Homologous quantities are E_m' and w' in the presence of Q_B^-. Expressing the potentials in millivolts and adopting 58 mV for $\ln(10)RT/F$, one has

$$w = \frac{10^{(E - E_m)/58}}{1 + 10^{(E - E_m)/58}} \tag{A6}$$

$$w' = \frac{10^{(E - E_m')/58}}{1 + 10^{(E - E_m')/58}} \tag{A7}$$

Assuming that no Q_B^- is present in the dark-adapted state and denoting z_1 the signal reflecting the flash-induced P^+ under reducing conditions, z_2 the signal at potential E, then w is measured as $(z_1 - z_2)/z_1$. We now consider an equilibrium situation with $[Q_B^-]$ centers in state Q_B^- and, noting T the total amount of RCs, $T - [Q_B^-]$ centers in state Q_B (meaning here all non-Q_B^- states). The amount of P^+ is then

$$[P^+] = w(T - [Q_B^-]) + w'[Q_B^-] = wT + [Q_B^-](w' - w) \tag{A8}$$

The first term is the amount of P^+ present in the dark, so that the increment of P^+ with respect to the baseline is

$$\Delta P^+ = [Q_B^-](w' - w) \tag{A9}$$

Using the experimentally measured ratio $y = \Delta P^+/[Q_B^-]$ one obtains

$$w' = y + w \tag{A10}$$

From eq A6, one derives

$$10^{E/58} = \frac{w}{1-w} 10^{E_m/58} \tag{A11}$$

which, inserted into eq A7 gives

$$w' = \frac{w 10^{-\Delta E_m/58}}{1 - w + w 10^{-\Delta E_m/58}} \tag{A12}$$

where $\Delta E_m = E'_m - E_m$. Inserting eq A12 into eq A10, rearranging and taking the log, one gets

$$\Delta E_m = -58 \log\left[\frac{(y+w)(1-w)}{w(1-y-w)}\right] \tag{A13}$$

Determination of $\Delta E_{m,P}$ in the Presence of Q_A^- under Steady-State Illumination. We consider the scheme

$$P^+Q_A \underset{o}{\overset{r}{\rightleftarrows}} PQ_A \underset{k}{\overset{J}{\rightleftarrows}} P^+Q_A^- \underset{o'}{\overset{r'}{\rightleftarrows}} PQ_A^-$$

The rate constants r and o relate to the interactions of P with the redox buffer for the Q_A state, r' and o' for the Q_A^- state. J is the rate of the photochemical conversion (depending on the illumination energy and on the trapping yield which is hyperbolically related to the amount of closed states because of excitonic connectivity of the antenna). k (abbreviating k_{PA}) is the recombination rate. Under steady-state conditions one has the equilibrium relations:

$$\frac{[P^+Q_A]}{[PQ_A]} = \frac{o}{r} \tag{A14}$$

$$\frac{[P^+Q_A^-]}{[PQ_A^-]} = \frac{o'}{r'}$$

The ratio o/r is determined as above by measuring the relative amount of photochemically active centers in the dark from the flash-induced changes of P. Using the notations of Figure 4, one has

$$\frac{o}{r} = \frac{z_1 - z_2}{z_2} \tag{A15}$$

We used two methods for determining o'/r'. The first one utilizes only the P^+ absorption changes, i.e., in addition to levels z_1 and z_2, levels z_3 (under steady-state illumination), and z_4 (flash induced level superimposed on the continuous illumination). The steady-state fraction of P^+ is

$$[P^+Q_A] + [P^+Q_A^-] = \frac{z_1 - z_2 + z_3}{z_1} \tag{A16}$$

We also have

$$[PQ_A] = \frac{z_4 - z_3}{z_1} \tag{A17}$$

and

$$[PQ_A^-] = \frac{z_2 - z_4}{z_1} \tag{A18}$$

Hence, using eqs A14 and A17

$$[P^+Q_A] = \frac{o}{r}\frac{z_4 - z_3}{z_1} \tag{A19}$$

Inserting into eqs A16 and using A15, one obtains

$$[P^+Q_A^-] = \frac{z_2(z_1 - z_2 + z_3) - (z_4 - z_3)(z_1 - z_2)}{z_1 z_2} \tag{A20}$$

Thus

$$\frac{o'}{r'} = \frac{[P^+Q_A^-]}{[PQ_A^-]} = \frac{z_2(z_1 - z_2 + z_3) - (z_4 - z_3)(z_1 - z_2)}{z_2(z_2 - z_4)} \tag{A21}$$

Finally,

$$\Delta E_m = -58 \log\left(\frac{o'r}{r'o}\right) = -58 \log\left[1 + \frac{z_1 z_3}{(z_1 - z_2)(z_2 - z_4)}\right] \tag{A22}$$

The second method uses the steady-state fraction $[Q_A^-]$ determined from the 742 nm absorption change (Figure 4C). Then, using eq A18

$$\frac{o'}{r'} = \frac{[P^+Q_A^-]}{[PQ_A^-]} = \frac{[Q_A^-] - [PQ_A^-]}{[PQ_A^-]} = \frac{z_1}{z_2 - z_4}[Q_A^-] - 1 \tag{A23}$$

The control experiment of Figure 3A, with ferrocene and ferrocyanide but without ferricyanide, shows that a small but significant steady-state amount of P^+ was reached under continuous illumination despite the reducing conditions, whereas our scheme predicts a zero steady-state level (a small effect of the superimposed flash is also discernible, showing that some RCs are in the PQ_A state). This nonzero level (which was saturated in the range of illumination energies that we used) is indicative of a slow leak through the stigmatellin block. Two processes may be responsible for this. The first possibility is the displacement of the inhibitor due to its k_{off} (rate of dissociation of the inhibitor on the Q_B pocket) and formation of the more stable state Q_B^-. As already mentioned, this phenomenon is reflected by the small slow phase observed in recombination kinetics (Figure 1). The centers where Q_B^- is thus formed are rapidly subject to a second photochemical turnover which resets them into the Q_B state with a high affinity for stigmatellin. We thus used a very high stigmatellin concentration (50 μM, i.e., more than 100 times the dissociation constant) to ensure rapid rebinding and minimize the accumulation of uninhibited centers. A second possibility is that oxidized ferrocene (or

ferricyanide, see ref *44*) could directly reoxidize Q_A^-. If such were the case, this phenomenon would be enhanced under oxidizing conditions and could distort the results.

When such a leak from states PQ_A^- and $P^+Q_A^-$ is introduced in the above model (with different rate constants, φ and φ', for each process), analytical expressions can still be derived, showing that an exact determination of o'/r' requires the independent measurement of the ratio φ'/r'. On the other hand, it appears that while expressions A21 and A23 both overestimate the value of o'/r', the distortion is much smaller with the latter formula. Hence, the experimental convergence of both expressions, as in the experiment of Figure 4, is a reliable test that the effect of the leak is negligible. It actually took us some time to design conditions where this criterion is met. A significant leak was indeed present when the incubation in the presence of ferricyanide and ferrocene was long, especially at large ferri/ferrocyanide ratios.

REFERENCES

1. Lancaster, C. R. D., Ermler, U., and Michel, H. (1995) in *Anoxygenic Photosynthetic Bacteria* (Blankenship, R. E., Madigan, M. T., and Bauer, C. E., Eds.) pp 503−526, Kluwer Academic Publishers, Dordrecht.
2. Noks, P. P., Lukashev, E. P., Kononenko, A. A., Venediktov, P. S., and Rubin, A. B. (1977) *Mol. Biol. (Moscow) 11*, 1090−1099.
3. Kleinfeld, D., Okamura, M. Y., and Feher, G. (1984) *Biochemistry 23*, 5780−5786.
4. Brzezinski, P., Okamura, M. Y., and Feher, G. (1992) in *The Photosynthetic Bacterial Reaction Center II* (Breton, J., and Verméglio, A., Eds.) pp 321−330, Plenum Press, New York.
5. Wraight, C. A. (1981) *Isr. J. Chem. 21*, 348−354.
6. Stein, R. R., Castellvi, A. L., Bogacz, J. P., and Wraight, C. A. (1984) *J. Cell. Biochem. 24*, 243−259.
7. Stowell, M. H. B., McPhillips, T. M., Rees, D. C., Soltis, S. M., Abresch, E., and Feher, G. (1997) *Science 276*, 812−816.
8. Lancaster, C. R. D. (1998) *Biochim. Biophys. Acta 1365*, 143−150.
9. Grafton, A. K., and Wheeler, R. A. (1999) *J. Phys. Chem. B 103*, 5380−5387.
10. Crofts, A. R., and Wraight, C. A. (1983) *Biochim. Biophys. Acta 726*, 149−185.
11. Kleinfeld, D., Okamura, M. Y., and Feher, G. (1984) *Biochim. Biophys. Acta 766*, 126−140.
12. Takahashi, E., and Wraight, C. A. (1992) *Biochemistry 31*, 855−866.
13. Labahn, A., Paddock, M. L., McPherson, P. H., Okamura, M. Y., and Feher, G. (1994) *J. Phys. Chem. 98*, 3417−3423.
14. Labahn, A., Bruce, J. M., Okamura, M. Y., and Feher, G. (1995) *Chem. Phys. 197*, 355−366.
15. Allen, J. P., Williams, J. C., Graige, M. S., Paddock, M. L., Labahn, A., Feher, G., and Okamura, M. Y. (1998) *Photosynth. Res. 55*, 227−233.
16. McPherson, P. H., Okamura, M. Y., and Feher, G. (1988) *Biochim. Biophys. Acta 934*, 348−368.
17. Maroti, P., and Wraight, C. A. (1988) *Biochim. Biophys. Acta 934*, 314−328.
18. Baciou, L., Sinning, I., and Sebban, P. (1991) *Biochemistry 30*, 9110−9116.
19. Lavergne, J., Matthews, C., and Ginet, N. (1999) *Biochemistry 38*, 4542−4552.
20. Wraight, C. A. (1979) *Biochim. Biophys. Acta 548*, 309−327.
21. McComb, J. C., Stein, R. R., and Wraight, C. A. (1990) *Biochim. Biophys. Acta 1015*, 156−171.
22. Kleinfeld, D., Abresch, E. C., Okamura, M. Y., and Feher, G. (1984) *Biochim. Biophys. Acta 765*, 406−409.
23. Shopes, R. J., and Wraight, C. A. (1985) *Biochim. Biophys. Acta 806*, 348−356.
24. Vermeglio, A., and Clayton, R. K. (1977) *Biochim. Biophys. Acta 461*, 159−165.
25. Jenney, F. E., and Daldal, F. (1993) *EMBO J. 12*, 1283−1292.
26. Rott, M. A., Witthuhn, V. C., Schilke, B. A., Soranno, M., Abdulfatah, A., and Donohue, T. J. (1993) *J. Bacteriol. 175*, 358−366.
27. Vermeglio, A. (1977) *Biochim. Biophys. Acta 459*, 516−524.
28. Joliot, P., Béal, D., and Frilley, B. (1980) *J. Chim. Phys. 77*, 209−216.
29. Joliot, P., and Joliot, A. (1984) *Biochim. Biophys. Acta 765*, 210−218.
30. Verméglio, A. (1982) in *Function of quinones in energy conserving systems* (Trumpower, B. L., Ed.) pp 169−180, Academic Press, New York.
31. Tiede, D. M., Utschig, L., Hanson, D. K., and Gallo, D. M. (1998) *Photosynth. Res. 55*, 267−273.
32. Lancaster, C. R. D., and Michel, H. (1999) *J. Mol. Biol. 286*, 883−898.
33. Miksovska, J., Kalman, L., Schiffer, M., Maroti, P., Sebban, P., and Hanson, D. K. (1997) *Biochemistry 36*, 12216−12226.
34. Baciou, L., Bylina, E. J., and Sebban, P. (1993) *Biophys. J. 65*, 652−660.
35. Gilson, M. K., and Honig, B. (1986) *Biopolymers 25*, 2097−2119.
36. Antosiewicz, J., and McCammon, J. A. (1996) *Biochemistry 35*, 7819−7833.
37. Alexov, E. G., and Gunner, M. R. (1999) *Biochemistry 38*, 8253−8270.
38. Krishtalik, L. I. (1996) *Biochim. Biophys. Acta 1273*, 139−149.
39. Shinkarev, V. P., and Wraight, C. A. (1997) *Biophys. J. 72*, 2304−2319.
40. Allen, J. P., Lous, E. J., Feher, G., Chirino, A., Komiya, H., and Rees, D. C. (1990) in *Current Research in Photosynthesis* (Baltscheffsky, M., Ed.) pp 61−64, Kluwer Academic Publishers, Dordrecht.
41. Johnson, G. N., Rutherford, A. W., and Krieger, A. (1995) *Biochim. Biophys. Acta 1229*, 202−207.
42. Krieger, A., and Rutherford, A. W. (1997) *Biochim. Biophys. Acta 1319*, 91−98.
43. Krieger, A., Rutherford, A. W., and Jegerschold, C. (1998) *Biochim. Biophys. Acta 1364*, 46−54.
44. Shopes, R. J., and Wraight, C. A. (1986) *Biochim. Biophys. Acta 848*, 364−371.

BI001588P